Proc. Natl. Acad. Sci. USA
Vol. 92, pp. 2333–2337, March 1995
Biochemistry

HypB protein of *Bradyrhizobium japonicum* is a metal-binding GTPase capable of binding 18 divalent nickel ions per dimer

(hydrogenase/metalloprotein/nitrogen fixation)

CHANGLIN FU, JONATHAN W. OLSON, AND ROBERT J. MAIER

Department of Biology, Johns Hopkins University, Baltimore, MD 21218

Communicated by Saul Roseman, Johns Hopkins University, Baltimore, MD, November 28, 1994

ABSTRACT **_Bradyrhizobium japonicum hypB_ encodes a protein containing an extremely histidine-rich region (24 histidine residues within a 39-amino-acid stretch) and guanine nucleotide-binding domains. The product of the _hypB_ gene was overexpressed in _Escherichia coli_ and purified by Ni^{2+}-charged metal chelate affinity chromatography (MCAC) in a single step. In SDS/PAGE, HypB migrated at 38 kDa—slightly larger than the calculated molecular mass (32.8 kDa). Purified HypB has GTPase activity with a k_{cat} of 0.18 min^{-1} and a K_m for GTP of 7 μM, and it has dGTPase activity as well. HypB exists as a dimer of molecular mass 78 kDa in native solution as determined by fast protein liquid chromatography on Superose 12. It binds 9.0 ± 0.14 divalent nickel ions per monomer (18 Ni^{2+} per dimer) with a K_d of 2.3 μM; it also binds Zn^{2+}, Cu^{2+}, Co^{2+}, Cd^{2+}, and Mn^{2+}. In-frame deletion of the histidine-rich region (deletion of 38 amino acids including 23 histidine residues) resulted in a truncated HypB that did not bind to the MCAC column, whereas in-frame deletion of 14 amino acids including 8 histidine residues within HypB resulted in a truncated HypB that still bound to the column. The results indicate that the histidine residues within the histidine-rich region of HypB are involved in metal binding.**

Nitrogen-fixing prokaryotes have the ability to reduce atmospheric N_2 to NH_3, termed biological N_2 fixation. Nitrogen fixation by rhizobia, in association with leguminous plants (such as alfalfa, clover, beans, peas, and soybeans), occurs in the specialized nodules on the plant roots; this allows the plants to grow well without added expensive nitrogenous fertilizers. The reduction of N_2 to NH_3 is catalyzed by the metalloenzyme nitrogenase. The nitrogenase reaction is very energy intensive, usually requiring between 16 and 42 ATP molecules per N_2 reduced. In addition to reduction of N_2 to form NH_3, nitrogenases from all known sources catalyze an ATP-dependent H_2 evolution reaction, and this H_2 production is an inherent property of the nitrogenase reaction. About 25–35% of the total energy required for the nitrogenase reaction is committed to reduce protons to form H_2 (1), representing a significant loss of energy. However, some N_2-fixing symbionts possess an uptake hydrogenase that is capable of oxidizing the nitrogenase-evolved hydrogen. This process thereby regenerates ATP via a membrane-bound respiratory electron-transport chain and makes the overall nitrogen-fixing process more energy efficient. Moreover, the scavenging of O_2 via H_2 oxidation prevents O_2-mediated damage to nitrogenase.

Bradyrhizobium japonicum, the N_2-fixing symbiont of soybean plants, synthesizes a Ni^{2+}-containing uptake-type hydrogenase. The purified enzyme contains two subunits (2, 3), and the structural genes for hydrogenase have been sequenced (4). Ni^{2+}, O_2, and H_2 have been found to be involved in hydrogenase gene regulation at the transcriptional level (5, 6). In addition to the hydrogenase structural genes, there are at least 19 genes identified within the hydrogenase gene cluster that have been shown or suggested to be involved in hydrogenase activity (7–12). Of particular interest is the *hypB* gene that in *B. japonicum* encodes a protein with an extremely histidine-rich region at the N terminus from His-16 through His-54 (i.e., HAHDHHHDHGHDHDHGHDGHHHHHHGHDQ-DHHHHHDHAH; see Table 1) and guanine nucleotide-binding domains conserved in GTP-binding proteins (G proteins) (8). Similar *hypB* genes have been reported to occur in a number of hydrogenase-containing bacteria (13–18). Based on the deduced amino acid sequences of *hypB* genes in these bacteria, all HypB proteins contain GTP-binding domains and a variable number of histidine residues (ranging from 10 to 26) clustered at the N terminus; one exception is *E. coli* HypB, which does not contain clustered histidine residues at the N terminus. Nevertheless, purified HypB from *E. coli* has a GTPase activity, but no Ni^{2+} binding to the purified protein was demonstrated (19). Very recently, Rey *et al.* (20) have also purified HypB from the pea symbiont, *Rhizobium leguminosarum*, and demonstrated that the purified HypB was able to bind 3.9 divalent nickel ions per monomer. GTPase activity was unable to be demonstrated in this protein probably due to the aggregation of HypB (20). Here, we report the purification and biochemical properties of HypB from *B. japonicum* expressed in *E. coli*. *B. japonicum* HypB is a metal-binding protein that has GTPase activity and binds 18 Ni^{2+} per dimer. A preliminary report of this work was presented at the Fourth International Conference on the Molecular Biology of Hydrogenases, August 14–19, 1994, Noordwijkerhout, The Netherlands.

MATERIALS AND METHODS

Bacterial Strain and Growth Conditions. *E. coli* BL21(DE3) (21), which carries a chromosomally encoded gene for a phage T7 RNA polymerase, was used for protein expression. *E. coli* HB101 and DH5α (GIBCO/BRL) were used for routine genetic manipulations. *E. coli* strains were grown on Luria–Bertani (LB) medium.

Construction of Plasmid pET-hypB for the Regulated Overexpression of *hypB*. To clone the *hypB* gene into the expression vector pET-21a(+) (Novagen), an ≈1.0-kb *Acc* I fragment harboring the entire *hypB* gene isolated from pKS2.5E2 (8) (Fig. 1) was blunted and cloned into the *Sma* I-digested pBluescript II KS(+) vector (Stratagene) (the 5′-end of the *hypB* gene is proximal to the *Pst* I site of the vector); this yielded pKS-hypB. Two synthesized oligonucleotides creating an *Nde* I site and the N-terminal portion of *hypB* were annealed and cloned into *Sal* I/*Pst* I double-digested pKS-hypB, forming pKS-hypB* (see Fig. 1). An ≈1.0-kb *Nde* I–*Not* I fragment was then isolated from pKS-hypB* and directionally cloned into

The publication costs of this article were defrayed in part by page charge payment. This article must therefore be hereby marked "*advertisement*" in accordance with 18 U.S.C. §1734 solely to indicate this fact.

Abbreviations: *hyp*, gene(s) encoding hydrogenase-related function with pleiotropic phenotype; MCAC, metal chelate affinity chromatography; IPTG, isopropyl β-D-thiogalactoside; FPLC, fast protein liquid chromatography; G protein, GTP-binding proteins.

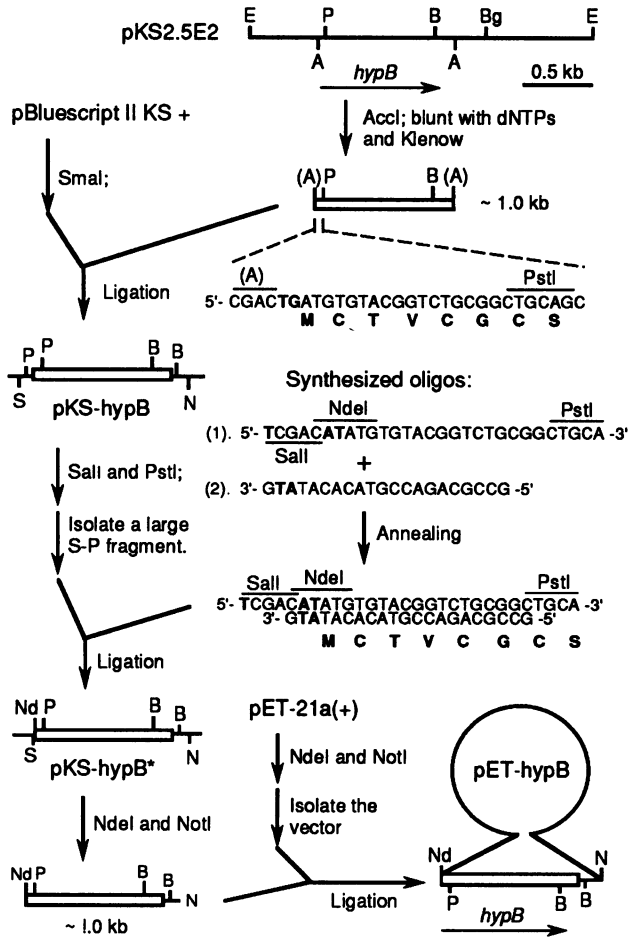

FIG. 1. Cloning strategy of the *hypB* gene into the expression vector pET-21a(+). A, *Acc* I; B, *Bam*HI; Bg, *Bgl* II; E, *Eco*RI; Nd, *Nde* I; N, *Not* I; P, *Pst* I; S, *Sal* I. Restriction enzyme sites in parentheses indicate the sites that have been modified in the course of cloning and cannot be cut by these enzymes. Not all restriction sites are shown on plasmids.

Nde I/*Not* I double-digested pET-21a(+); this resulted in pET-hypB (Fig. 1).

Overexpression and Purification of the HypB Protein from *E. coli*. To express the HypB protein, plasmid pET-hypB harboring the *hypB* gene was transformed into *E. coli* strain BL21(DE3) (21). Strain BL21(DE3) carrying pET-hypB was grown at 37°C in 1 liter of LB medium containing 100 μg of ampicillin per ml in 2-liter flasks with shaking at 220 rpm to an OD_{600} ≈1.0; isopropyl β-D-thiogalactopyranoside (IPTG) was added to a final concentration of 0.2 mM. After further incubation for 2 hr with shaking at 37°C, the cells were harvested at 8000 × *g* for 10 min at 4°C. All subsequent steps were carried out at 4°C unless otherwise stated. The cell pellet was washed once with 50 mM Tris acetate (TA) buffer (pH 8.25) and resuspended in ≈15–20 ml of fresh buffer. The cells were broken by two passages through a French press cell at 12,000 psi (1 psi = 6.89 kPa) in the presence of 1 mM phenylmethylsulfonyl fluoride and a small amount of DNase A. The lysate (crude extract) was centrifuged at 12,000 × *g* for 10 min to pellet unbroken cells. The cell-free extract was further centrifuged at 115,000 × *g* for 1.5 hr. The supernatant was used as the source for further purification of HypB.

To purify HypB, a metal chelate affinity chromatography (MCAC) (iminodiacetic acid-conjugated agarose) column (Sigma) was used. The column was loaded with 3–4 ml of 0.1 M $NiCl_2$ in water and washed with 4 column volumes of 50 mM TA buffer, pH 8.25/0.5 M NaCl. The supernatant containing HypB was then loaded onto the column, and the flow-through was collected. The column was then washed with a large volume (20–30 column volumes) of TA buffer, pH 8.25/0.5 M NaCl (or 0.6 M NaCl). The bound HypB protein was subsequently eluted with the same buffer containing 10 mM EDTA. Eluted fractions (2-ml fractions) were collected and checked by SDS/PAGE to determine purity. Pure fractions were pooled and dialyzed three times against 2 liters of 50 mM TA buffer (pH 8.25) to remove the EDTA, salt, and Ni^{2+}. The dialyzed protein (referred to as "purified HypB") was then used for biochemical and enzymological experiments. Protein concentration was initially determined by using the BCA Protein Assay Kit (Pierce) with bovine serum albumin as the standard. For accurate determination of Ni^{2+} per monomer, purified protein was also quantitated directly by amino acid composition analysis.

Amino Acid Analysis and Determination of Molecular Size. The N-terminal amino acid sequencing of the purified HypB was carried out on an Applied Biosystems model 478 protein sequencer, and amino acid composition analysis was done with the Pico·Tag system (Waters) at the Protein/Peptide/DNA Facility of The Johns Hopkins University School of Medicine. The native molecular mass of HypB was determined by gel filtration chromatography at 25°C on an FPLC Superose 12 10/30 column (Pharmacia) as described (22), except that sample (HypB) and protein size standards were dissolved in 50 mM TA buffer (pH 8.25). The same buffer was used for column equilibration and protein elution.

Metal-Binding Assay. Binding of Ni^{2+} by purified HypB was determined by equilibrium dialysis vs. 1 liter of 50 mM TA, pH 8.25/50 mM NaCl containing different amounts of $NiCl_2$ (as indicated in Fig. 3) for 48 hr. A 2-ml sample of 5–6 μM HypB was contained in the dialysis bag (cutoff point, 12,000 kDa). Binding of other metals, such as Zn^{2+}, Cu^{2+}, Co^{2+}, Cd^{2+}, Ca^{2+}, Mg^{2+}, and Mn^{2+}, by HypB was assayed similarly. Metal content was determined by atomic absorption (flame) spectrophotometry as described (23). Each reading reported by the instrument was an average of four determinations. The maximum Ni^{2+} content of HypB (9.0 ± 0.14) is based on the average of five points ± SD from saturating Ni^{2+}-binding conditions.

Measurement of GTPase Activity. GTP-hydrolyzing activity was measured by two methods, colorimetric and radioactive assays. For the time-course assay, the reaction mixture (1.2 ml) containing 50 mM Tris chloride (pH 7.5), 50 mM KCl, 5 mM $MgCl_2$, 1 mM dithiothreitol (19), 2 mM GTP, and 7 μM HypB was incubated at 37°C. Aliquots (200 μl) were removed at different incubation times as indicated and added to 200 μl of a 20% charcoal (Norit A) suspension (acid washed; pH 4.5) and incubated at 4°C for 5 min. The sample was centrifuged for 5 min at 12,000 × *g*. PO_4^{3-} was determined by the method of Ames and Dubin (24). The ability of HypB to hydrolyze ATP, CTP, UTP, and dGTP was determined similarly to that described for GTP.

To determine the K_m for GTP, assay was performed in 100 μl of reaction mixture (in the same buffer as above) containing various concentrations (0.2–10 μM) of [γ-^{32}P]GTP and 0.1 μM HypB. After 10 min of incubation at 37°C, the reaction was terminated as described above. The $^{32}PO_4^{3-}$ in the supernatant was quantitated by liquid scintillation spectrometry.

RESULTS

Expression in *E. coli* and One-Step Purification of the *B. japonicum* HypB. From analyzing the nucleotide sequence, the *hypB* gene was cloned into an expression vector, pET-21a(+), by creating an *Nde* I site at the position of the initiator methionine (5′ end) (see Fig. 1). The resulting plasmid pET-hypB carrying the *hypB* gene under the control of the phage T7ϕ10 promoter has a strong ribosome-binding site. It was transformed into *E. coli* BL21(DE3) carrying a chromosomally encoded gene for a IPTG-inducible phage T7 RNA poly-

merase to facilitate expression as described in *Materials and Methods.* Clearly, HypB is the major protein overexpressed upon IPTG induction (Fig. 2).

The presence of 24 histidine residues at the N terminus of HypB was highly suggestive that the protein could bind Ni^{2+} with strong affinity; therefore Ni^{2+}-charged MCAC was used to purify this protein. The supernatant fraction of a cell-free extract from the induced culture of *E. coli* BL21(DE3) carrying pET-hypB was loaded on a Ni^{2+}-charged MCAC column and eluted with buffer containing EDTA. In the absence of an *in vitro* assay for HypB protein, column fractions were analyzed by SDS/PAGE to evaluate protein purity. Despite its high level of expression, the HypB protein did not apparently reside in inclusion bodies but was maintained in a soluble form in the supernatant (see Fig. 2, lane 3). Most *E. coli* proteins did not bind to the affinity column and were contained in the column flow-through fraction (Fig. 2, lane 4). Under the optimized purification conditions as described herein, the eluted fractions contained primarily the HypB protein (with the exception of the first two fractions after the start of the EDTA elution, data not shown). The pure fractions were pooled and analyzed by SDS/PAGE. This revealed no contaminating bands (Fig. 2, lane 5). The results show that the *B. japonicum* HypB protein has a strong binding affinity for Ni^{2+}, an ability that greatly facilitates a simplified purification of the protein at a rather high yield: about 50 mg of protein was recovered from 1 liter of culture. This yield accounts for about 20–25% of the total protein loaded onto the column.

On SDS/PAGE, HypB migrated at ≈38 kDa, which is slightly larger than the calculated molecular mass of 32.8 kDa. This is similar to the *R. leguminosarum* HypB, which migrates as a 39-kDa band in SDS/PAGE, also larger than the calculated value of 32 kDa (20).

Amino Acid Analysis and Determination of Native Molecular Size. Purified HypB was used to determine the N-terminal amino acid sequence. With the exception of the initiator methionine, the obtained sequence (Xaa-Thr-Val-Xaa-Gly-Xaa-Ser-Asp-Gly-Lys-Ala) corresponded exactly to that from the deduced amino acid sequence of *hypB* (Met-Cys-Thr-Val-Cys-Gly-Cys-Ser-Asp-Gly-Lys-Ala). The N-terminal methionine is apparently cleaved from the protein. Total amino acid composition analysis indicated that the molar percent composition for each amino acid also corresponded well with that predicted from the gene sequence (data not shown).

The native molecular size of the purified HypB was determined by gel filtration on a calibrated FPLC column. Although some large molecular mass proteins were eluted early (perhaps aggregates of HypB), a major peak eluting at a position corresponding to a size of ≈78 kDa (data not shown) indicated that HypB under native conditions is probably a homodimer. This is similar to *E. coli* HypB, which also exists as a homodimer under native conditions (19).

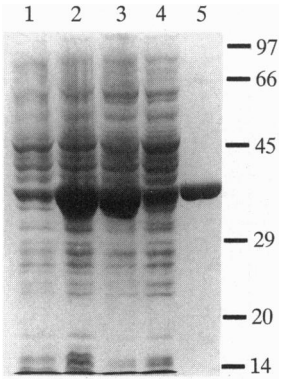

FIG. 2. SDS/PAGE analysis of the expression and purification of HypB. Samples from *E. coli* BL21(DE3) carrying the plasmid pET-hypB were subjected to SDS/12.5% PAGE, and the gel was stained with Coomassie blue. Lanes: 1, crude extract from cells without IPTG; 2, crude extract from cells with IPTG induction; 3, supernatant; 4, flow-through from the Ni^{2+}-charged MCAC column after loading supernatant; 5, purified HypB (pooled fractions without the first two fractions) from the column.

Ni^{2+} Binding by Purified HypB. To determine the Ni^{2+}-binding capacity of HypB, the pure protein was dialyzed against 50 mM TA buffer (pH 8.25) containing different amounts of Ni^{2+}. Equilibrium dialysis experiments demonstrated that HypB was able to bind 9.0 ± 0.14 Ni^{2+} per monomer (thus 18 Ni^{2+} per dimer) (Fig. 3). At the concentration of HypB used (6.4 μM) and conditions employed here, the binding of HypB to Ni^{2+} reached saturation at 10–20 μM Ni^{2+} in solution. From these data, an apparent K_d of ≈2.3 μM was calculated.

Binding of Other Metals by HypB. Since HypB strongly binds Ni^{2+}, the ability of HypB to bind other metals was of interest. Notably, by both qualitative (MCAC column) and quantitative (atomic absorption analysis after equilibrium dialysis) procedures, HypB also bound Zn^{2+}, Cu^{2+}, Co^{2+}, and Cd^{2+} but not Ca^{2+} or Mg^{2+} (data not shown). HypB has approximately the same affinity for Zn^{2+} as for Ni^{2+} (data not shown). Based on the equilibrium dialysis approach for testing Mn^{2+}-binding and subsequent atomic absorption analyses, HypB also bound to Mn^{2+}, but it did not bind tightly to Mn^{2+}-charged MCAC column. This latter result is probably due to the loose interaction of Mn^{2+} with the column at the pH used, rather than to a weak binding affinity of HypB for Mn^{2+}.

Expression of the Truncated HypB. To establish that the clustered multiple histidine residues within HypB are involved in the metal-binding properties, in-frame deletions of the *hypB* gene within the histidine-rich region were constructed (see Table 1). The two truncated HypB proteins were expressed in *E. coli* BL21(DE3), and their metal-binding abilities were then examined. The truncated HypB lacking 38 amino acids of which 23 are histidine residues (Table 1) did not bind to the Ni^{2+}-charged MCAC column (Fig. 4*A*) or to the other metal-charged columns, such as Zn^{2+}, Cu^{2+}, Co^{2+}, and Cd^{2+} (data not shown). The results indicate that the histidine-rich region of HypB is clearly important for metal binding. Notably, in-frame deletion of 14 amino acids, including 8 histidine residues within HypB (Table 1), resulted in a truncated version of HypB that still bound to the Ni^{2+}-charged column (Fig. 4*B*), indicating that the histidine residues remaining in the truncated HypB are sufficient to permit Ni^{2+} binding.

GTPase Activity. Based on the deduced amino acid sequence, HypB contains potential guanine nucleotide-binding motifs that are conserved in a large number of G proteins (26). GTP-hydrolyzing activity was measured as described in *Materials and Methods.* Fig. 5 shows a time course and kinetic study of GTPase activity of HypB. Clearly, purified HypB

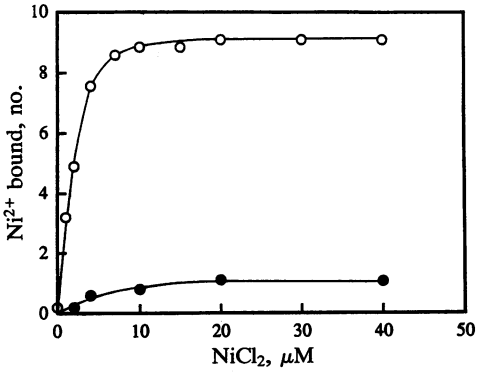

FIG. 3. Ni^{2+} binding of HypB based on equilibrium dialysis. ○, HypB; ●, bovine serum albumin (BSA) as a control. BSA has been shown (25) to bind one Ni^{2+} per molecule.

Table 1. Amino acid sequences at the N termini of HypB and truncated HypB

Plasmid	Gene	Amino acids at the N terminus	Total AA
		1 10 20 30 40 50 56	
pET-hypB	*hypB*	(M) CTVCGCSDGKASIEHAHDHHHDHGHDHDHGHDGHHHHHHGHDQDHHHHHDHAHGX	302
		18	
pET-ΔhypB23	*ΔhypB23*	(M) CTVCGCSDGKASIE----------HGX	264
		42	
pET-ΔhypB8	*ΔhypB8*	(M) CTVCGCSDGKASIEHAHDHHHDHGHDHDHGHDGHHHHH----------HGX	288

Residue numbers refer to the deduced amino acid sequence for the full-length protein. The N-terminal methionine (in parentheses) was found to be removed from the wild-type protein, as determined by protein microsequencing. The dashed lines indicate the amino acids that were deleted in the truncated HypB. Plasmids pET-ΔhypB23 and pET-ΔhypB8 were constructed through a series of subcloning steps. Appropriate restriction enzymes (i.e., *Dsa* I and *Pst* I, or *Dsa* I only) were used to delete the histidine-rich region encoded within the *hypB*. Two synthesized oligonucleotides (5′-GCGACGGCAAGGCGTCCATCGAA-3′ and 3′-ACGTCGCTGCCGTTCCGCAGGTAGCTTGTGC-5′) were used to facilitate the construction of pET-ΔhypB23. The expected sequence yielded for all constructs was verified by DNA sequencing.

showed a significant level of GTPase activity (Fig. 5*A*). Analysis of the results indicates that HypB has a GTPase activity with a k_{cat} of 0.18 min^{-1}, similar to the *E. coli* HypB (k_{cat} of 0.17 min^{-1}) (19), and the calculated K_m for GTP was ≈7 μM (Fig. 5*B*). HypB also hydrolyzed dGTP, but not ATP, CTP, or UTP (data not shown). The k_{cat} determined by the colorimetric method (which measures total phosphate) (24) was in good agreement with the k_{cat} (0.18 min^{-1}) determined by the radioactive assay with [γ-^{32}P]GTP (measuring orthophosphate). These results are suggestive that HypB hydrolyzes GTP into the products GDP and orthophosphate. Interestingly, we found during our analysis that purified HypB (as isolated from *E. coli*) contains a mixture of bound guanine nucleotides as determined by HPLC (27) with a total stoichiometry of 1:1, relative to the monomer protein (data not shown).

DISCUSSION

B. japonicum HypB has been successfully overexpressed in *E. coli* and purified in a single step by using MCAC. Purified HypB showed significant GTPase and dGTPase activities. It was able to bind 9 Ni^{2+} per monomer and thus 18 Ni^{2+} per dimer. It also bound other metal ions, such as Zn^{2+}, Cu^{2+}, Co^{2+}, Cd^{2+}, and Mn^{2+}. To our knowledge, such a high Ni^{2+}-binding capacity for a protein has not been documented from any biological source.

Because of the presence of a histidine-rich region (24 histidine residues) clustered at the N terminus of HypB, purification of HypB was readily achieved by means of a Ni^{2+}-charged MCAC column. This method is based on the Ni^{2+}-charged matrix (iminodiacetic acid-agarose), which has a strong affinity for proteins or peptides with a few contiguous histidines (28, 29). A similar column (Ni^{2+}–nitrilotriacetic acid-agarose column) has been used to purify *R. leguminosarum* HypB (20). The fact that in-frame deletion of the histidine-rich region (including 23 histidine residues) resulted in a truncated version of *B. japonicum* HypB that did not bind the metal-charged column indicates that the clustered histidine residues within HypB are involved in metal binding. Notably,

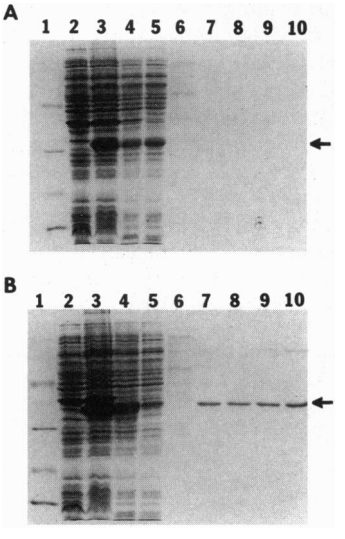

FIG. 4. Expression and SDS/PAGE analysis of two truncated derivatives of HypB. (*A*) Samples from strain BL21(DE3) carrying the plasmid pET-ΔhypB23 (see Table 1). (*B*) Samples from strain BL21 (DE3) carrying the plasmid pET-ΔhypB8 (see Table 1). Lanes: 1, molecular mass standards (from the top to the bottom: 96, 66, 45, 29, 20, and 14 kDa, respectively); 2, crude extract without IPTG; 3, crude extract after IPTG induction; 4, supernatant; 5, flow-through from the Ni^{2+}-charged column; 6–10, elution fractions from the column. The truncated versions of HypB were expressed in the same way as for wild-type HypB.

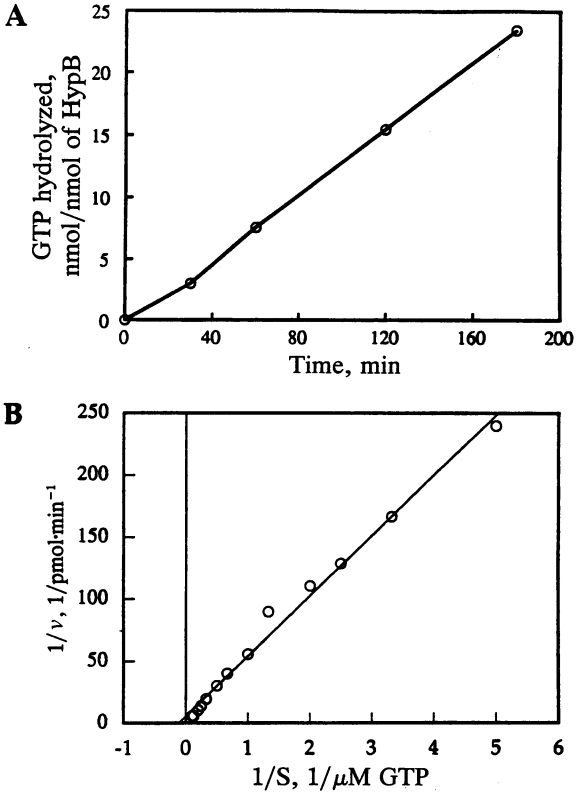

FIG. 5. Kinetics of GTPase activity of HypB. (*A*) Time course of GTPase activity of HypB. (*B*) Lineweaver–Burk plot [reciprocal velocity *v* vs. reciprocal substrate (S) concentration] from which K_m and k_{cat} were calculated.

deletion of 14 amino acids (including 8 histidine residues) within the histidine-rich region did not affect the binding of the truncated HypB to the Ni^{2+}-charged column, indicating that there are still enough histidine residues available for liganding Ni^{2+}. Successful purification of HypB by this method without denaturing the protein also suggests that the histidine residues within HypB are solvent-exposed for their interaction with metals.

B. japonicum HypB is capable of binding 9 Ni^{2+} per monomer. This is in contrast to the *R. leguminosarum* HypB (which binds 3.9 Ni^{2+} per monomer) (20), although *R. leguminosarum* HypB has almost the same number of histidine residues near its N terminus as *B. japonicum* HypB. The differences in Ni^{2+}-binding are perhaps due to differences in the number of histidine residues available for interaction with the metal. In addition, the UreE protein from *Klebsiella aerogenes* has a histidine-rich stretch (10 histidines of 15 amino acid residues) at the C terminus and has been shown to bind 3 Ni^{2+} per monomer (6 Ni^{2+} per dimer) (30). *E. coli* HypB does not bind Ni^{2+} in solution, probably because of the absence of a histidine-rich region within it (19). Both *B. japonicum* HypB and *E. coli* HypB (19) exist as dimers, whereas *R. leguminosarum* HypB seems to form a complex of unknown subunit stoichiometry (20). .

Purified recombinant *B. japonicum* HypB showed a GTPase activity with a k_{cat} of 0.18 min^{-1} and dGTPase activity, but not ATPase, CTPase, or UTPase activities, suggesting that the enzyme is specific for the hydrolysis of GTP. It is likely that the enzyme (HypB) is not able to discriminate dGTP from GTP, since their structures are similar. The HypB GTPase activity is quite low compared with most GTPases and G proteins (26) but is similar to *E. coli* HypB (19). Signal transduction type G proteins are involved in "switch mechanisms" in which various intracellular and transmembrane signals involved with a great diversity of biological processes can be amplified or activated by binding GTP, and these processes are subsequently inactivated by the hydrolysis of GTP to GDP (26). The products of the *hypB* genes apparently play roles that are clearly different from these G proteins. In *E. coli*, HypB appears to be directly involved in Ni^{2+} donation to the hydrogenase apoprotein since the *hypB*$^-$ mutant accumulated the precursor form of hydrogenase 3, which was devoid of Ni^{2+} (19, 31). Very recently, Maier and Böck (†) demonstrated that a mutation in domain G1 of *E. coli* HypB caused the strain to synthesize normal amounts of the mutated HypB (with decreased GTP binding and hydrolysis) but had no hydrogenase activity. Based on the characterization of *E. coli* HypB, it is reasonable to speculate that *B. japonicum* HypB together with other products is involved in some step(s) of Ni^{2+} incorporation into a hydrogenase or a precursor; GTP hydrolysis may be required for efficient Ni^{2+} transfer.

The strong metal-binding capacity of *B. japonicum* HypB implicates a role for HypB as a metal sponge or sink that may provide metal ions for subsequent metal-containing enzymes when needed. It is noteworthy that the products of the *hypB* genes from soil bacteria (including *B. japonicum, R. leguminosarum, Azotobacter vinelandii, Azotobacter chroococcum*, and *Alcaligenes eutrophus*) have clustered multiple histidine residues, which may bind multiple atoms of divalent metals. Such proteins may have evolved because of commonly encountered metal-poor soil conditions.

We are grateful to James Kolonay, David Frick, Krista Lowe, and Allan Stone for assistance with FPLC, GTPase assays, HPLC analysis, and atomic absorption spectrophotometry experiments, respectively, and Wu-Schyong Liu for amino acid analysis. We thank Fred Moshiri, Maurice Bessman, Richard McCarty, Norman Meadow, and Saul Roseman for suggestions. This work was supported by Department of Energy Grant DE-FG0289ER14011.

1. Eisbrenner, G. & Evans, H. J. (1983) *Annu. Rev. Plant Physiol.* **34,** 105–136.
2. Arp, D. J. (1985) *Arch. Biochem. Biophys.* **237,** 504–512.
3. Stults, L. W., Moshiri, F. & Maier, R. J. (1986) *J. Bacteriol.* **166,** 795–800.
4. Sayavedra-Soto, L. A., Powell, G. K., Evans, H. J. & Morris, R. O. (1988) *Proc. Natl. Acad. Sci. USA* **85,** 8395–8399.
5. Kim, H. & Maier, R. J. (1990) *J. Biol. Chem.* **265,** 18729–18732.
6. Kim, H., Yu, C. & Maier, R. J. (1991) *J. Bacteriol.* **173,** 3993–3999.
7. Van Soom, C., Verreth, C., Sampaio, M. J. & Vanderleyden, J. (1993) *Mol. Gen. Genet.* **239,** 235–240.
8. Fu, C. & Maier, R. J. (1994) *Biochem. Biophys. Acta* **1184,** 135–138.
9. Fu, C. & Maier, R. J. (1994) *Gene* **141,** 47–52.
10. Fu, C. & Maier, R. J. (1994) *Gene* **145,** 91–96.
11. Fu, C., Javedan, S., Moshiri, F. & Maier, R. J. (1994) *Proc. Natl. Acad. Sci. USA* **91,** 5099–5103.
12. Black, L., Fu, C. & Maier, R. J. (1994) *J. Bacteriol.* **176,** 7102–7106.
13. Dernedde, J., Eitinger, M. & Friedrich, B. (1993) *Arch. Microbiol.* **159,** 545–553.
14. Tibelius, K. H., Du, L., Tito, D. & Stejskal, F. (1993) *Gene* **127,** 53–61.
15. Chen, J. C. & Mortenson, E. (1992) *Biochim. Biophys. Acta* **1131,** 199–202.
16. Lutz, S., Jacobi, A., Schlensog, V., Böhm, R., Sawers, G. & Böck, A. (1991) *Mol. Microbiol.* **5,** 123–135.
17. Rey, L., Murillo, J., Hernando, Y., Hidalgo, E., Cabrera, E., Imperial, J. & Ruiz-Argüeso, T. (1993) *Mol. Microbiol.* **8,** 471–481.
18. Colbeau, A., Richaud, P., Toussaint, B., Caballero, F. J., Elster, C., Delphin, C., Smith, R. L., Chabert, J. & Vignais, P. M. (1993) *Mol. Microbiol.* **8,** 15–29.
19. Maier, T., Jacobi, A., Sauter, M. & Böck, A. (1993) *J. Bacteriol.* **175,** 630–635.
20. Rey, L., Imperial, J., Palacios, J.-M. & Ruiz-Argüeso, T. (1994) *J. Bacteriol.* **176,** 6066–6073.
21. Studier, F. W. & Moffatt, B. A. (1986) *J. Mol. Biol.* **189,** 113–130.
22. Ferber, D. M. & Maier, R. J. (1993) *FEMS Microbiol. Lett.* **110,** 257–264.
23. Maier, R. J. & Fu, C. (1994) *Biometals* **7,** 279–286.
24. Ames, B. N. & Dubin, D. T. (1960) *J. Biol. Chem.* **235,** 769–775.
25. Glennon, J. D. & Sarkar, B. (1982) *Biochem. J.* **203,** 15–23.
26. Bourne, H. R., Sanders, D. A. & McCormick, F. (1991) *Nature (London)* **349,** 117–127.
27. Moal, J., Le Coz, R., Samain, J. F. & Daniel, J. Y. (1989) *Comp. Biochem. Physiol. B* **93,** 307–316.
28. Porath, J., Carlsson, J., Olsson, I. & Belfrage, G. (1975) *Nature (London)* **258,** 598–599.
29. Hochuli, E., Bannwarth, W., Döbeli, H., Gentz, R. & Stüber, D. (1988) *Biotechnology* **6,** 1321–1325.
30. Lee, M. H., Pankratz, H. S., Wang, S., Scott, R. A., Finnegan, M. G., Johnson, M. K., Ippolito, J. A., Christianson, D. W. & Hausinger, R. P. (1993) *Protein Sci.* **2,** 1041–1052.
31. Jacobi, A., Rossmann, R. & Böck, A. (1992) *Arch. Microbiol.* **158,** 444–451.

†Maier, T. & Böck, A., Fourth International Conference on the Molecular Biology of Hydrogenases, Aug. 14–19, 1994, Noordwijkerhout, The Netherlands, pp. 90–91.